Journal Pre-proof

North Korean CO emissions reconstruction using DMZ ground observations, TROPOMI space-borne data, and the CMAQ air quality model

Eunhye Kim, Byeong-Uk Kim, Hyun Cheol Kim, Yang Liu, Yoon Hee Kang, Daniel J. Jacob, Yong Pyo Kim, Jung-Hun Woo, Jhoon Kim, Shuxiao Wang, Chul Yoo, Changhan Bae, Younha Kim, Soontae Kim

Please cite this article as: E. Kim, B.-U. Kim, H.C. Kim, et al., North Korean CO emissions reconstruction using DMZ ground observations, TROPOMI space-borne data, and the CMAQ air quality model, *Science of the Total Environment* (2023), https://doi.org/10.1016/j.scitotenv.2024.171059

North Korean CO Emissions Reconstruction Using DMZ Ground Observations, TROPOMI Space-Borne Data, and the CMAQ Air Quality Model

Eunhye Kim[a, b], Byeong-Uk Kim[c], Hyun Cheol Kim[d,e], Yang Liu[b], Yoon Hee Kang[a], Daniel J. Jacob[f], Yong Pyo Kim[g], Jung-Hun Woo[h], Jhoon Kim[i], Shuxiao Wang[j], Chul Yoo[k], Changhan Bae[k], Younha Kim[l], Soontae Kim[a, b, *]

[a]Department of Environmental & Safety Engineering, Ajou University, Suwon 16499, Republic of Korea

[b]Gangarosa Department of Environmental Health, Rollins School of Public Health, Emory University, Atlanta, GA 30322, USA

[c]Georgia Environmental Protection Division, Atlanta, GA, 30354, USA

[d]Air Resources Laboratory, National Oceanic and Atmospheric Administration, College Park, MD, 20740, USA

[e]Cooperative Institute for Satellite Earth System Studies, University of Maryland, College Park, MD, 20740, USA

[f]School of Engineering and Applied Sciences, Harvard University, Cambridge, MA, 02138, USA

[g]Department of Chemical Engineering and Materials Science, Ewha Womans University, Seoul 03760, Republic of Korea

[h]Department of Civil and Environmental Engineering, Konkuk University, Seoul, 05029, Republic of Korea

[i]Department of Atmospheric Sciences, Yonsei University, Seoul, 03722, Republic of Korea

Abbreviations: CAPSS, Clean Air Policy Support System; CMAQ, Community Multi-Scale Air Quality; CNEMC, China National Environmental Monitoring Centre; DMZ, Demilitarized Zone; EI, emissions inventory; IOA, index of agreement; NAIR, National Air Emission Inventory and Research Center; NIER, National Institute of Environmental Research; SIJAQ, Satellite Integrated Joint Monitoring of Air Quality; SMA, Seoul metropolitan area; TROPOMI, TROPOspheric Monitoring Instrument; VCD, vertical column density

jState Key Joint Laboratory of Environment Simulation and Pollution Control, School of

Environment, Tsinghua University, Beijing 100084, China

kEmission Inventory Management Team, National Air Emission Inventory and Research

Center, Cheongju, 28166, Republic of Korea

lDepartment of Energy, Climate, and Environment, International Institute for Applied

Systems Analysis, Laxenburg 2361, Austria

Corresponding author: Soontae Kim

Email: soontaekim@ajou.ac.kr

Abstract

Emission uncertainty in North Korea can act as an obstacle when developing air pollution management plans in the country and neighboring countries when the transboundary transport of air pollutants is considered. This study introduces a novel approach for adjusting and reallocating North Korean CO emissions, aiming to complement the limited observational and emissions data on the country's air pollutants. We utilized ground observations from demilitarized zone (DMZ) and vertical column density (VCD) data from a TROPOspheric Monitoring Instrument (TROPOMI), which were combined with the Community Multi-Scale Air Quality (CMAQ) chemistry transport model simulations. The Clean Air Support System (CAPSS) and Satellite Integrated Joint Monitoring of Air Quality (SIJAQ) emissions inventories served as the basis for our initial simulations. A two-step procedure was proposed to adjust both the emission intensity and the spatial distribution of emissions. First, air quality simulations were conducted to explore model sensitivity to changes in North Korean CO emissions with respect to ground concentrations. DMZ observations then constrained these simulations to estimate corresponding emission intensity. Second, the spatial structure of North Korean CO emission sources was reconstructed with the help of TROPOMI CO VCD distributions. Our two-step hybrid method outperformed individual emissions adjustment and spatial reallocation based solely on surface or satellite observations. Validation using ground observations from the Chinese Dandong site near the China-North Korea border revealed significantly improved model simulations when applying the updated CO emissions. The adjusted CO emissions were 10.9 times higher than those derived from the bottom-up emissions used in this study, highlighting the lack of information on North Korean pollutants and emission sources. This approach offers an efficient and practical solution for identifying potential missing emission sources when there is limited on-site information about air quality on emissions.

Keywords: North Korea, Vertical Column Density, Air Quality Model, Emissions Adjustment, Spatial Allocation

1. Introduction

In North Korea, the annual mortality rate due to air pollution is 207.2 persons per 100,000 people, the highest worldwide (WHO, 2020). This is attributable to high personal exposure to air pollutants due to poor fuel use with coal and solid biofuels as well as insufficient air pollution control devices (Kim et al., 2019a; Kim et al., 2019b; Yeo et al., 2018). For example, CO emissions, an indicator of incomplete combustion (Feng et al., 2020), are estimated to be 2.7 times higher in North Korea than those in South Korea (Yeo et al., 2019). Considering that NOx emissions in North Korea account for only 24% of those in South Korea (Bae et al., 2018; Kim et al., 2014), the severely high concentrations of air pollutants, including CO emissions, caused by low-quality fuel consumption and lack of emission control in North Korea, are significant.

As North Korea does not release an official emissions inventory (EI), emissions in North Korea have been estimated with limited data, such as electric power generation and consumption, from a report submitted to the United Nations Environment Programme (Woo et al., 2003). As bottom-up emissions are generally estimated based on the emission factors and activities for target emission sources, collecting accurate information on emission sources is crucial (Kurokawa et al., 2020; Li et al., 2017; Woo et al., 2020). Information on North Korean emission sources, however, is not easily accessible. Moreover, acquiring air pollutant concentration observations often used to indirectly verify estimated emissions is difficult. Therefore, estimated emissions in North Korea are expected to have higher uncertainty than those of neighboring countries (Kim et al., 2014; Yeo et al., 2019).

The emissions uncertainty in North Korea can trigger appreciable concerns as regional source-receptor relationships should be considered to alleviate air pollution for the neighboring countries. This includes the establishment of appropriate air pollution control policies, air quality forecasts, and the analysis of health effects related to air pollutants (Crippa et al., 2019; Egerstrom et al., 2023; Lee et al., 2020; Lim et al., 2020; Oh et al., 2023). Therefore, it is essential to use realistic emissions from North Korea for air quality research in Northeast Asia.

Previous studies have adjusted bottom-up emissions using in-situ ground observations and air quality simulations (Bae et al., 2020; Kim et al., 2021; Kim et al., 2024). However, this approach is not applicable because ground observation data in North Korea are unavailable. The air quality of North Korea has been estimated using the suburban monitoring stations in South Korea and at North Korea–China border sites (Choi et al., 2020; Pendergrass et al., 2022). Nevertheless, emissions in North Korea have not yet been quantitatively assessed.

In response to the growing social interest in air pollution, the number of air quality monitoring stations in South Korea increased from 260 in 2016 to 504 in 2021. Among these stations, the air pollutant concentrations at the newly installed monitoring stations along the demilitarized zone (DMZ) in the vicinity of North Korea (hereafter, "DMZ monitoring stations") are expected to be significantly affected by the air pollutants transported from North Korea depending on wind patterns. Estimating emissions in North Korea will be possible if their contributions can be separated from ground observations at the DMZ monitoring stations (hereafter, "DMZ observations"). A recent study estimated transboundary air pollutants using observations at a downwind monitor in Northeast Asia (Itahashi et al., 2022; Jo et al., 2020; Kang et al., 2023); however, there is little research on North Korea.

A few studies have estimated relative changes in emissions in North Korea using the top-down method based on satellite-observed vertical column density (VCD) data (Chong et al., 2023; Kim et al., 2014); however, the emission intensity was not directly estimated. Recently, observational data on CO VCD over North Korea were used to identify the local hotspot areas, including large point sources (Chong et al., 2023). They estimated the spatial distribution of North Korean CO emissions using CO VCD from Measurement of Pollution In The Troposphere (MOPITT). For pollutants such as CO, which have a long residence time in the atmosphere, horizontal and vertical concentration distributions may vary significantly depending on meteorological conditions (Cho et al., 2022; Kim et al., 2023; Lee et al., 2019). Thus, directly estimating CO emission rates from specific emission sources on the ground is still challenging using VCD data (Kong et al., 2022; Xia et al., 2016).

Herein, a method to adjust emission intensity and its spatial distribution of CO in North Korea was developed by combining DMZ observations, an air quality simulation with an existing EI, and satellite observations. The emissions adjustment and spatial reallocation method was validated by comparing CO concentrations re-simulated with the adjusted emissions to the observations from DMZ and the North Korea–China border area. This method can be applicable if observations close to the target area are available. Furthermore, the method can be used to accurately perform numerical air quality forecasts and to better develop air quality improvement policies by securing reliable emissions in a study area of interest.

2. Materials and Methods

Emissions adjustment and reallocation of CO emissions for North Korea in a bottom-up EI were primarily carried out using two main approaches (Figure 1):

i. Ground observation-based approach: North Korean CO emissions were adjusted based on ground observations, followed by spatial reallocation using the EI and (or) satellite VCD data (see Section 2.3).

ii. Satellite observation-based approach: North Korean CO emissions in the EI were spatially reallocated based on satellite CO VCD, followed by emissions adjustment using ground observations or satellite VCD data (see Section 2.4).
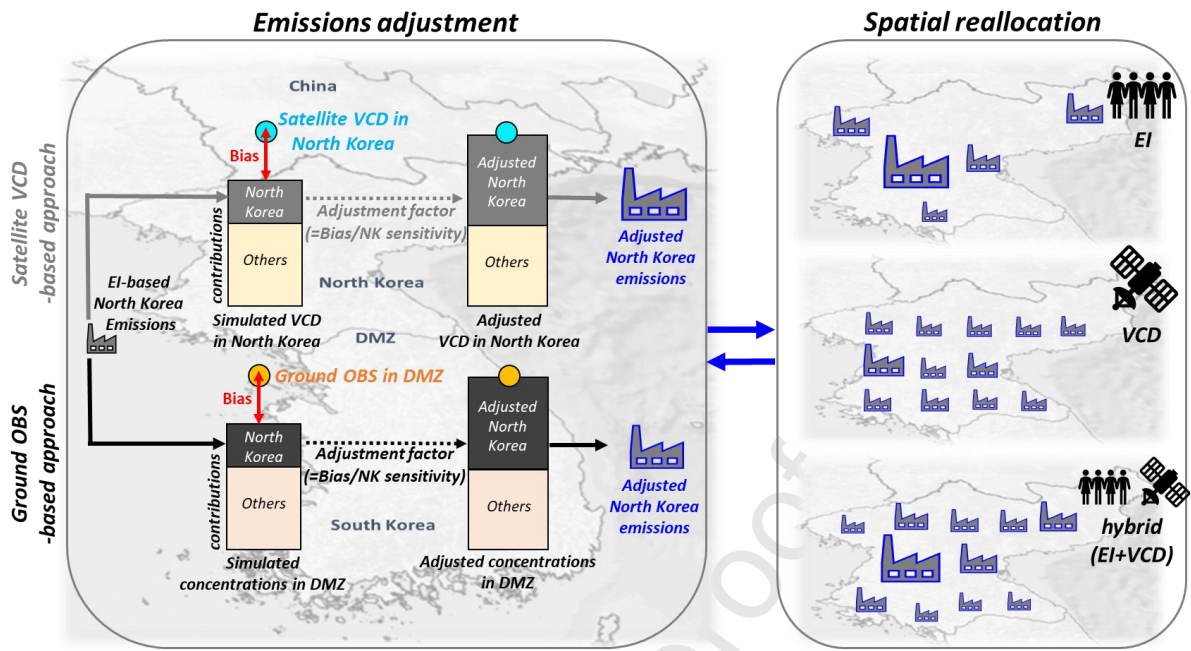
Figure 1. Conceptual diagram for adjusting and reallocating emissions in North Korea. EI; emissions inventory, DMZ; demilitarized zone, NK; North Korea, VCD; vertical column density.

Table 1 shows the emissions scenario description for North Korea in this study. Details of each emissions adjustment and spatial reallocation are explained in Sections 2.3 and 2.4. General descriptions of the procedures are provided as the Supplementary Data.

Table 1. Emissions adjustment and spatial reallocation methods tested in this study to update CO emissions in North Korea.

Case	Emissions adjustment	Spatial reallocation	Description
BASE	Not applied	Not applied	Pre-gridded bottom-up emissions inventory (EI)-based emissions (adjusted for China and South Korea except the DMZ area)
Ground observation-based approach (ADJ1-ADJ3) Step 1 (common): Adjusting the total CO emissions in North Korea based on the BASE emissions and DMZ ground observations.			
ADJ1	DMZ observations	Not applied	The spatial distribution of the emissions remains the same as in the BASE.
ADJ2		TROPOMI VCD	Step 2: Reallocating the ADJ1 emissions at the provincial level using the spatial distribution of satellite VCD.
ADJ3		EI & TROPOMI VCD	Step 2: Reallocating the ADJ1 emissions at the provincial level using a hybrid method that incorporates both spatial distributions of BASE emissions and satellite VCD.

7

Satellite observation-based approach (ADJ4-ADJ6) Step 1 (common): Emissions in the BASE were primarily reallocated based on the spatial distribution of satellite VCD data			
ADJ4	DMZ observations	TROPOMI VCD	Step 2: Adjusting North Korean total CO emissions based on DMZ ground observations.
ADJ5	TROPOMI VCD		Step 2: Adjusting North Korean total CO emissions based on the observed to modeled VCD ratio.
ADJ6	TROPOMI VCD and DMZ observations		Step 2: Adjusting North Korean total CO emissions based on the observed to modeled VCD ratio. Step 3: Re-adjusting CO emissions, which were adjusted in Step 2, based on DMZ ground observations.

2.1. Observational data

The Meteorological Assimilation Data Ingest System measurement data provided by the National Centers for Environmental Prediction were used to evaluate the meteorological simulation results. The meteorological data from two monitoring stations in Northeast China and thirty-two stations in South Korea were available inside the modeling domain. To verify simulated CO concentrations, air quality monitoring data from 224 monitoring stations of the China National Environmental Monitoring Centre (CNEMC; http://www.cnemc.cn/en/) in Northeast China and 473 stations of the National Institute of Environmental Research (NIER) AirKorea (https://www.airkorea.or.kr) in South Korea were available for our study area.

Among the stations in South Korea, averaged data from seven DMZ monitoring stations were used to evaluate and adjust CO emissions in North Korea (Figure 2). All stations near the DMZ were newly installed in 2019 and 2020. As there are no residential areas with civilians in the DMZ, we assumed that DMZ monitoring stations are located in the background area of South Korea. In addition, the Civilian Control Zone (CCZ), approximately 5 to 10 km long, functions as a buffer zone to limit anthropogenic emissions in the country, excluding those from the military sector. Although a couple of sites are close to the urban areas, the CO emission density of the seven monitoring stations is approximately 15% of the national average of South Korea (8.17 tons/year/km^2). However, notably, emissions from military facilities are not currently available in the emissions inventory. Once included, they may have appreciable impacts on simulated CO concentrations and thus, the emissions adjustment. In addition, geographically, North Korea is located north of the DMZ monitoring stations,

8

and we assumed that the impact of CO emissions in South Korea on the monitoring stations can be minimized when northerly winds are prevailing and that the increase in North Korean CO emissions would have an effect. CO concentrations at the DMZ stations are 172 ppb (30%) lower than those at the Seoul Metropolitan Area (SMA), which is close to the DMZ stations. This shows that those monitoring stations serve as background monitoring stations for South Korea.

For adjusted emission cross-validation, four ground stations in Dandong, China, located near the North Korea–China border (hereafter "Dandong monitoring stations") were additionally used (left box in Figure 2). Air pollutants transported from North Korea can also affect them depending on wind direction. Regarding ground observation concentrations, 1-hour average observation data from each station were averaged to calculate the daily average for subsequent analysis. If missing values accounted for more than 8 hours a day, the observation data for that day were not utilized. Figure 2 shows the locations of the ground monitoring stations used to adjust emissions in North Korea.
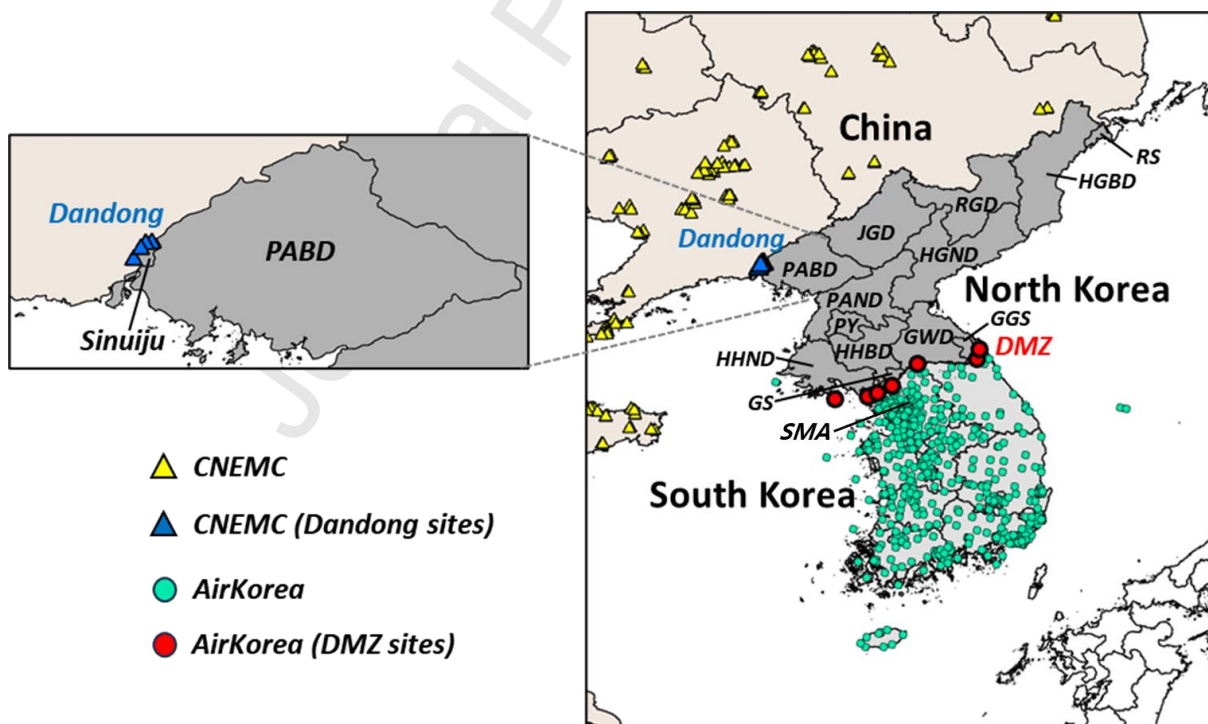
Figure 2. The simulation area and monitoring stations used in this study. There are 13 provinces in North Korea: Rason (RS), Hamgyongbukdo (HGBD), Hamgyongnamdo (HGND), Ryanggangdo

(RGD), Jagangdo (JGD), Pyonganbukdo (PABD), Pyongannamdo (PAND), Pyongyang (PY), Hwanghaenamdo (HHND), Hwanghaebukdo (HHBD), Gaesung (GS), Gangwondo (GWD), and Geumgangsan (GGS). The blue and yellow triangles indicate China National Environmental Monitoring Centre (CNEMC) monitoring stations in Northeast China. The blue triangles represent monitoring stations in Dandong, China. The green and red circles indicate the Airkorea monitoring stations of National Institute of Environmental Research (NIER) in South Korea. The red circles represent monitoring stations along the DMZ in South Korea.

For the spatial reallocation of emissions in North Korea, a Sentinel-5P TROPOspheric Monitoring Instrument (TROPOMI) carbon monoxide CO column 1-Orbit L2 VCD was used (https://disc.gsfc.nasa.gov/datacollection/S5P_L2__CO_____HiR_1.html). The spatial resolution of the data was 5.5 km × 7 km. Only data with the quality assurance flag qa=1 were utilized.

2.2. Air quality simulation

This study focused on the air quality of North Korea in winter (December 2020 to March 2021) when fuel consumption was high due to the increased use of heating applications. During this period, northwesterly winds become predominant; thus, emissions in North Korea may significantly affect the air quality in South Korea more in winter than in other seasons (Bae et al., 2018; Choi et al., 2020; Kim et al., 2022). To calculate the contributions of North Korean emissions to CO concentrations at the DMZ monitoring stations, the simulation results from the Community Multi-scale Air Quality (CMAQ) model version 5.3.2, a photochemical model, were used. The simulation was conducted in a 9-km grid resolution domain, including the Korean Peninsula. Boundary conditions were obtained from the re-simulated air pollutant concentrations by utilizing adjusted emissions for China and South Korea, which can affect North Korean air quality in Northeast Asia, according to Kim et al. (2024). Among the input data for CMAQ, the meteorology data were prepared using Weather Research and Forecasting (WRF) version 3.9.1 based on the Final Analysis (FNL) of the National Centers for Environmental Prediction. Biogenic emissions were calculated using the Model of Emissions of Gases

and Aerosols from Nature (MEGAN; Guenther et al., 2006) version 2.1.

Clean Air Policy Support System (CAPSS) 2021, provided by the National Air Emission Inventory and Research Center (NAIR), was used as a bottom-up EI for South Korea. The Sparse Matrix Operator Kernel Emission (SMOKE) version 4.8 model was used for its spatiotemporal allocation and chemical speciation. Satellite Integrated Joint Monitoring of Air Quality (SIJAQ) v2, a monthly pre-gridded EI developed by Konkuk University, was used for the rest of Northeast Asia, including North Korea and China. SIJAQv2 had been developed for the year 2017 to support the GEMS Map of Air Pollution (GMAP) field measurement campaign and updated from the previous version. The anthropogenic EI was generated based on CREATE (Comprehensive Regional Emissions Inventory for Atmospheric Transport Experiments; Woo et al, 2020) and the LTP (the Joint Research Project for Long–range Transboundary Air Pollutants in Northeast Asia) emissions inventories. The emissions were estimated using the Greenhouse Gas and Air Pollution Interactions and Synergies-Asia (GAINS-Asia) model (http://gains.iiasa.ac.at). Activity data for the energy-related sectors were obtained mostly from World Energy Balance statistics produced by the International Energy Agency (https://www.iea.org/data-and-statistics). Non-energy activity data were collected from the database of the GAINS framework (http://gains.iiasa.ac.at) and various international statistics such as ones provided by the UN Statistics Division (https://data.un.org/), World Bank (https://data.worldbank.org/), and FAOSTAT (Food and Agriculture Statistics, https://www.fao.org/faostat/en/#data). Emission factors and control efficiencies were taken from input parameters in GAINS-Asia. The EI includes CO, NH_3, NOx, $PM_{2.5}$, PM_{10}, SO_2, and VOCs emissions from anthropogenic sources, including marine shipping. The major six emission source categories in the EI are power sector, industrial combustion, industrial processes, mobile sources, solvent use, agricultural, and waste. For each source category, emissions are further divided by each sub-sector, fuel type, and end-of-pipe control device. They cover more than 50 fuel types and 20 sub-sectors. The horizontal extent of the EI geographically covers whole Asia. The Sparse Matrix Operator Kernel Emissions for Asia (SMOKE-Asia; Woo et al., 2012) was utilized to process the EI and prepare

CMAQ-ready emissions based on the SAPRC99 chemical mechanism (W. Carter, 1999). Because the base year of SIJAQv2 was 2017, the emissions could differ from those in 2021, the study period. Additionally, biomass burning, one of major sources of CO emissions, was not considered in the EI due to the lack of detailed available data for the country.

Given these limitations, before adjusting CO emissions in North Korea, CO emissions for China and South Korea where ground observation concentrations were available were adjusted using a method described by Kim et al. (2024). Figure S1 and Table S1 show the model performance evaluation (MPE) results for the simulated CO concentrations with the adjusted emissions in China and South Korea. The simulated CO concentration of China was 578 ppb before the emissions adjustment; however, it increased to 860 ppb after the Chinese emissions adjustment. Thus, the emissions adjustment reduced the difference from the observed concentration (833 ppb). The correlation coefficients (r) were similar before and after the Chinese emissions adjustment (0.74 and 0.72, respectively). The simulated CO concentration of South Korea was 237 ppb before the adjustment. However, after the South Korean emissions adjustment, it increased to 504 ppb, reproducing the observed concentration (508 ppb) well. In addition, the r value improved from 0.63 before adjustment to 0.97 after adjustment. The base simulation for our modeling domain (Figure 2) was then conducted based on these adjusted emissions (hereafter, "base emissions").

2.3. Ground observation-based approach

As depicted in Figure 1, CO emissions in North Korea can be adjusted based on ground observations along the DMZ. CO concentrations at DMZ monitoring stations can be affected by emissions in South Korea, North Korea, China, and other neighboring areas. Considering that emissions in areas other than North Korea were adjusted as described in Section 2.2, the discrepancy between the observed and simulated concentrations at the DMZ monitoring stations was assumed to be primarily attributable to the uncertainty in North Korean CO emissions. North Korean CO emissions can then be adjusted based on modeled CO sensitivity and the mean bias between observed and modeled concentrations as shown in Eq. (1), similar to Cooper et al. (2017) and Li et al. (2023).

They used NO_2 VCD to estimate recent changes in emissions with the formula. In Eq. (1), we utilized DMZ ground observations to adjust North Korean CO emissions instead of using space-borne observations.

$$E_{ADJ,G} = [(C_{OBS} - C_{BASE})/S + 1] \times E_{BASE} \quad (1)$$

where

$E_{ADJ,G}$: Adjusted CO emissions in North Korea based on DMZ ground observations

E_{BASE}: CO emissions in North Korea in base emissions

C_{OBS}: Observed CO concentrations at the DMZ ground monitoring stations

C_{BASE}: Simulated CO concentrations using base emissions (E_{BASE}) at the DMZ monitoring stations

S: Sensitivity of CO concentrations at the DMZ monitoring stations to relative change in CO emissions in North Korea (ppb)

S was calculated using the brute-force method, which calculates the sensitivity of modeled concentration before and after a relative emission perturbation rate ($=\Delta C/\Delta\varepsilon$) (see Supplementary Data). The perturbation rate ($\Delta\varepsilon$) of 0.5 was adopted in this study and uniformly applied to all grids in North Korea. Note that the term within the parentheses in Eq. (1) represents the emissions adjustment factor (γ) for North Korean emissions, aimed at minimizing the average difference between observed and simulated CO concentrations at DMZ monitoring stations each month. The obtained γ was then applied to adjust the monthly CO base emissions in North Korea (BASE in Table 1) in Step 1 of ADJ1-ADJ3 in Table 1.

Comprehensive environmental geographic information data, such as population distribution, road networks, and industrial complex locations, are used to develop surrogates for the spatial allocation during which emissions in irregular-shaped administrative districts are converted into gridded

13

emissions for Eulerian photochemical air quality simulation (Woo et al., 2020). Considering North Korea, however, the spatial distribution of emissions involves uncertainty because of limited population information for each city/province and the availability of energy and economic activity data. This indicates that base emissions have uncertainty not only in emissions intensity but also in their spatial distribution within North Korea. Therefore, if the same adjustment factor is applied to the pre-gridded EI emissions used in this study, the existing spatial allocation uncertainty of emissions is inherently reflected in the adjusted emissions.

The emissions in North Korea were reallocated using the horizontal distribution of TROPOMI VCD and(or) the spatial gradient of the pre-gridded emissions to make the spatial distribution of CO emissions in North Korea more realistic. Due to the inherent limitations in satellite observation and EI data, two methods (ADJ2 & ADJ3), as described in Table 1, were explored for the spatial reallocation of the emissions in this study (see Supplementary Data).

CO concentrations were re-simulated with the spatially reallocated emissions to validate the reallocation of CO emissions in North Korea. The simulation results were compared with the observations from the DMZ and Dandong monitoring stations (hereafter "Dandong observations"), which are close to North Korea. In addition, the modeled CO VCD was compared with TROPOMI VCD to check the spatial distribution and extent.

2.4 Satellite observation-based approach

Similar to the ground observations, satellite-observed VCD data can be utilized to adjust CO emissions in North Korea. In this approach, before adjusting CO emissions in North Korea, the pre-gridded bottom-up emissions were primarily reallocated based on the spatial distribution of observed CO VCD ($E_{Reallocated} = \sum E_{BASE} \times VCD_{TROPOMI} / \sum VCD_{TROPOMI}$) (see Supplementary Data). The reallocated emissions were used to further adjust emissions in ADJ4-ADJ6 in Table 1. We used Eq. (1) to adjust CO emissions in ADJ4. To adjust the CO emissions in ADJ5 and ADJ6, we utilized Eq. (2) with the ratio of observed to modeled CO VCD, incorporating the reallocated emissions ($E_{Reallocated}$)

14

and an averaged beta value (β) over North Korea. The methodology is similar to that of Lamsal et al. (2011) and Li et al. (2023). Monthly mean beta values were calculated using VCD values modeled with the bottom-up and adjusted emissions ($\beta = \Delta VCD / \Delta \varepsilon$).

$$E_{ADJ,S} = [(VCD_{TROPOMI} - VCD_{Model})/\beta + 1] \times E_{Reallocated} \quad (2)$$

where

$E_{ADJ,S}$: Adjusted CO emissions in North Korea based on satellite CO VCD data

$VCD_{TROPOMI}$: TROPOMI-observed CO VCD averaged in North Korea

VCD_{Model}: CO VCD modeled with $E_{Reallocated}$ averaged in North Korea

β: Sensitivity of modeled CO VCD to a relative change in CO emissions in North Korea (unitless)

$E_{Reallocated}$: Reallocated pre-gridded bottom-up CO emissions in North Korea based on TROPOMI CO VCD data

It is believed that the observed VCD was influenced not only by local emission impacts but also by regional transport due to the long residence time of CO (Kim et al., 2024; Zhou et al., 2021). Therefore, the discrepancy between observed and modeled VCDs can result from both local emissions and transported impact. However, when the VCD-based emissions adjustment is applied, all emission uncertainties are attributed solely to local emission sources in Eq. (2). In this study, CO emissions in BASE simulation were adjusted for China and South Korea. However, discrepancies in observed and simulated VCDs exist since the CO emissions adjustment was based on ground observations rather than satellite VCD data.

Further, satellite-observed VCD integrates all air pollutants throughout the entire atmospheric column, whereas regional air quality models, such as CMAQ used in this study, typically confine locally emitted air pollutants within the planetary boundary layer height (PBLH) (Byun and Schere 2006; Byun et al. 2007), which implies that the emissions adjustment in this study using satellite-

15

observed VCD may not fully resolve VCD differences throughout the entire column. Instead, this method modifies VCD within the PBLH to better match the observed VCD representing the whole column. As a result, the emissions adjustment for ADJ5, using TROPOMI CO VCD, may lead to overestimating CO emissions in North Korea. Recognizing this, we further adjusted the CO emissions in ADJ5 by applying the approach described in Section 2.3 to mitigate the overestimation, resulting in ADJ6 emissions.

3. Results and Discussion

3.1 Model performance before emissions adjustment

Before adjusting CO emissions in North Korea based on DMZ observations, MPE was conducted for meteorology and air quality simulations (BASE) in the modeling area that covers a part of China and South Korea. Figure S2 and Table S2 show that the 2-meter temperatures in Northeast China and South Korea were slightly underestimated, with mean biases of 0.0°C and -0.84°C, respectively. Meanwhile, the 10-meter wind speeds were slightly overestimated, with mean biases of 0.28 m/s and 0.45 m/s, respectively. In Northeast China and South Korea, index of agreement (IOA) values were both 0.99 for 2-m temperatures and 0.95 and 0.94 for 10-m wind speed, respectively, which met the benchmark criteria (2-m temperature: 0.8; 10-m wind speed: 0.6) proposed by Emery et al. (2001).

In the simulation results of CO concentrations (Figure 3), the correlation coefficients (r) for all monitoring stations in South Korea, Northeast China inside the modeling domain, the DMZ, and Dandong were as high as 0.98, 0.97, 0.84, and 0.69, respectively. However, the mean biases at the locations were −15.2, -20.5, −68.5, and −286.2 ppb, respectively. It can be noted that modeled CO concentrations underestimated those observed at all locations. However, the underprediction was most notable at the DMZ and Dandong monitoring stations in the border areas where North Korean CO emissions can have a substantial impact. Although CO emissions in Northeast China and South Korea were adjusted for the BASE simulation, the mean bias in the area near the DMZ still remained appreciable. The mean bias in this area was approximately 4.5 times higher than the average mean bias across South Korea. Therefore, the underestimated North Korean CO emissions in the BASE simulation apparently affected underpredictions of CO concentrations in the DMZ and Dandong.
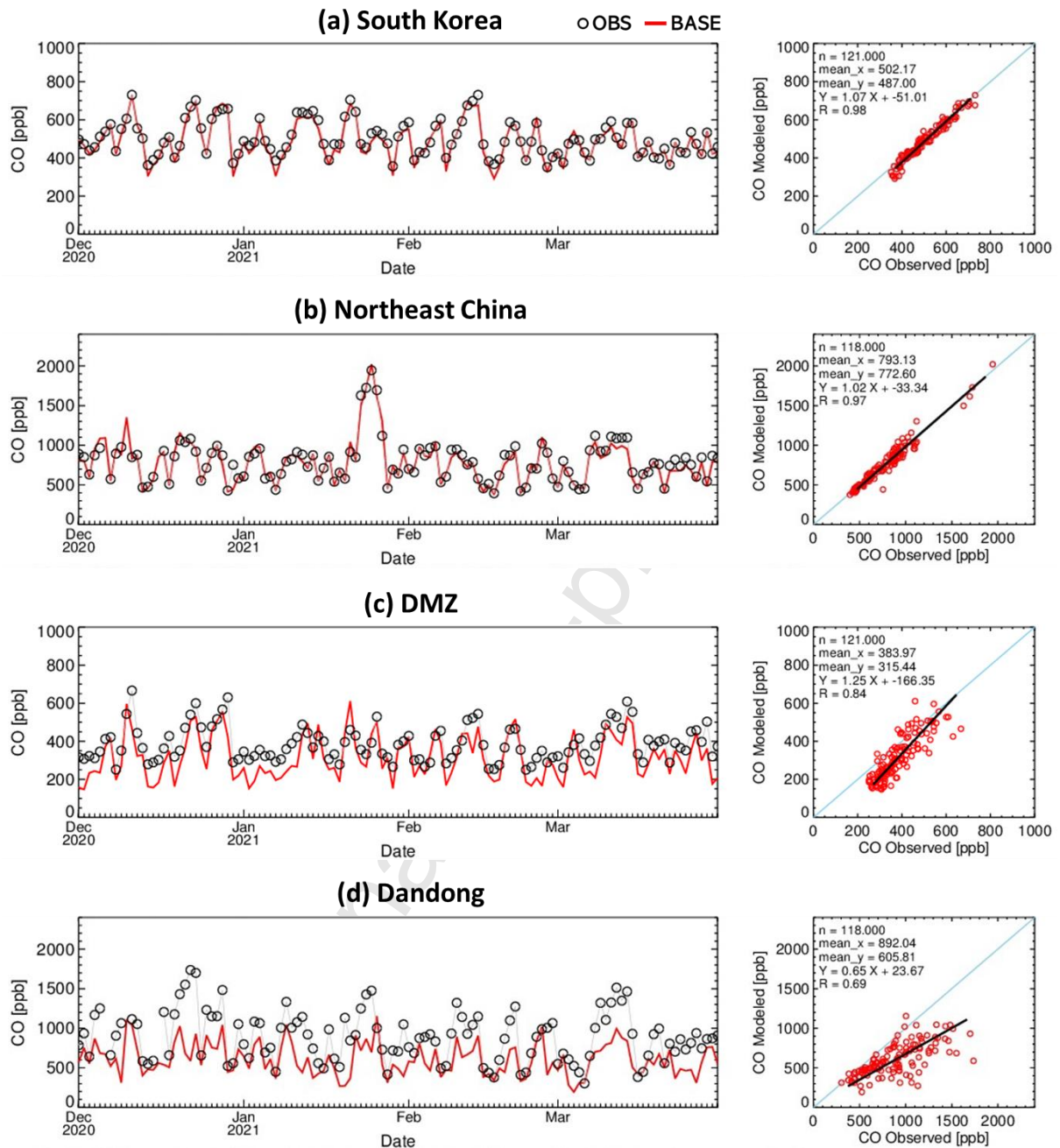
Figure 3. Model performance evaluation on daily averaged CO concentrations utilizing the BASE emissions for (a) South Korea, (b) DMZ, (c) Northeast China, and (d) Dandong monitoring stations during the simulation period of December 2020 to March 2021.

When comparing monthly CO VCD data, the modeled VCD for BASE simulation was consistently lower than the TROPOMI VCD (Figure S3). The discrepancy became pronounced in February when TROPOMI recorded the highest observed VCD for the month. On the other hand, in contrast to the first two months, the TROPOMI CO VCD averaged over North Korea increased by 10% during the last two months of the simulation period from December 2020 to March 2021. Note that CO

17

concentrations at the DMZ and Dandong monitoring stations decreased by 2% and 13%, respectively, during the last two months compared to the first two months (Figure 3), contrasting with the reverse tendency observed in the VCD change (Figure S3).

3.2 Comparisons of CO emissions adjustment

Before the emissions adjustment, monthly North Korean CO emissions in BASE were 69,656 metric tons per month (TPM) in December 2020, 68,495 TPM in January, 61,866 TPM in February, and 65,012 TPM in March 2021. After the emissions were adjusted using Eq. (1) following Step 1 for AJD1-ADJ3 as outlined in Table 1, the monthly CO emissions (ADJ1-ADJ3) amounted to 785,208 TPM in December, 623,520 TPM in January, 579,508 TPM in February, and 919,708 TPM in March (Figure 4). During the research period, North Korean CO emissions adjusted based on the ground observations were more than 10.9 times higher than those in the EI. The emission intensities in ADJ2 and ADJ3 are consistent with those in ADJ1.

When adjusted based on the DMZ observations following spatial reallocation using TROPOMI CO VCD data, the CO emissions (ADJ4) in North Korea increased by 8.2 compared to the EI. Monthly CO emissions in ADJ4 were 26% higher for December 2020 and 33% higher for January 2021 than those in ADJ1. However, they were 59% lower for February and 62% lower for March 2021. This contrast can be attributed to the distinct monthly variations between ground observations and TROPOMI VCD data during the simulation period. On the other hand, VCDs in North Korea increased during the last two months and exhibited relatively higher values in Pyongyang and the southwest area (Figure S3), where CO emissions can easily affect DMZ monitoring stations. These VCD increments during the last two months may reduce the magnitude of adjusted CO emissions when compared to those based on DMZ observations as well as those in the previous two months.

In addition to the emissions adjustments utilizing DMZ observations, we also attempted to spatially reallocate and then adjust North Korean CO emissions based on the ratio of the TROPOMI-observed to modeled CO VCDs as described in Section 2.4. Due to the significant differences between the modeled and observed CO VCDs over North Korea, as shown in Figure S4, it was estimated that CO emissions (ADJ5) in North Korea should be increased by 36.8 times compared to the EI emissions. Compared to the emissions adjustment utilizing DMZ observations, this increase was substantial and resulted in an overprediction of CO concentrations at DMZ monitoring stations as discussed in

18

Section 3.5.

To address this issue with the method described in Section 2.4, when CO emissions in ADJ5 were further adjusted based on DMZ observations, the total North Korean CO emissions increased by 14.8 times compared to the BASE emissions. It is worth noting that monthly emissions in ADJ6 significantly decreased when compared to those in ADJ5 and were only 24-66% higher than those in ADJ1.
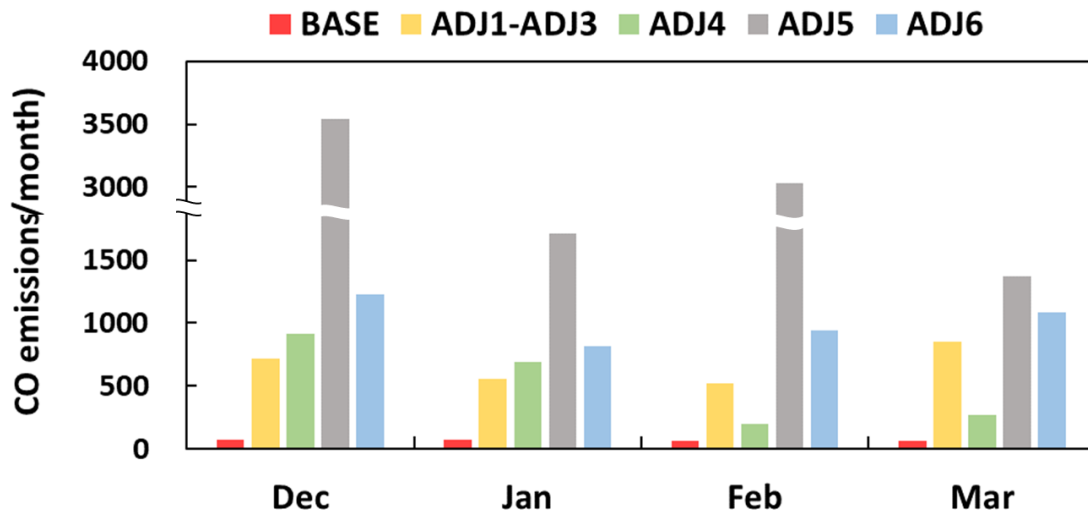
Figure 4. Monthly CO emission rates in North Korea before and after emissions adjustment from December 2020 to March 2021. The BASE represents CO emissions in the bottom-up emissions inventory. ADJ1-ADJ3 exhibits CO emissions adjusted utilizing the DMZ observations, while CO emissions in ADJ4 were first spatially reallocated and then adjusted based on DMZ observations. ADJ5 represents CO emissions spatially reallocated and adjusted based on TROPOMI VCD data, while CO emissions in ADJ6 were re-adjusted from those in ADJ5 based on the DMZ observations.

3.3 Spatial reallocation and distribution

Since a single emission adjusting factor for North Korea was applied, uncertainty embedded in the spatial allocation of pre-gridded emissions can be inherently reflected in the adjusted emissions (Figure 5). Specifically, if emissions allocated to specific grids are substantial in the pre-gridded base emissions, the spatial allocation issue can be exacerbated by applying a relatively large emission adjusting factor, as discussed in Section 3.2.
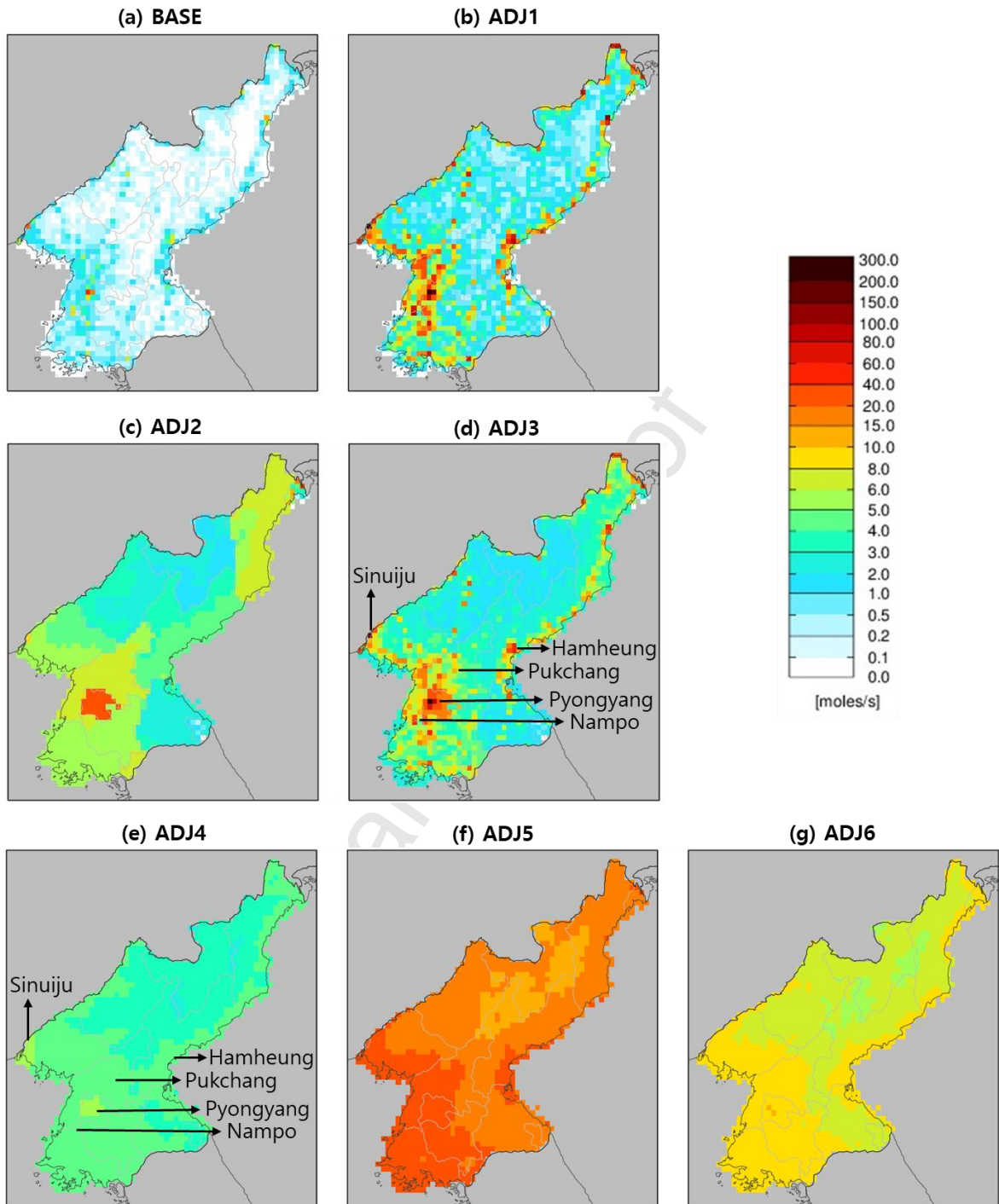
Figure 5. Spatial distributions of CO emissions in North Korea during the period of December 2020 to March 2021: (a) BASE and (b) ADJ1 with the spatial allocation as in the pre-gridded emissions. The TROPOMI VCD was used for spatial reallocations of (c) ADJ2, (e) ADJ4, (f) ADJ5, and (g) ADJ6, a hybrid method that incorporates both spatial distributions of the EI emissions, and the TROPOMI VCD was used for (d) ADJ3.

20

Screening of CO emissions for a total of 1,548 grids that cover North Korea (Figure 6) shows that the emissions are concentrated in specific grids in North Korea. For example, emissions before the adjustment for one single grid that corresponds to the Sinuiju area (Figure 2) accounted for 5% of the total emissions in North Korea, which appears unrealistic. Unlike large emission sources, such as power plants and industrial complexes, there is little information on emission sources in suburban and agricultural areas with relatively lower emissions. In such areas, the base emissions were evaluated as relatively low. Thus, the change in emissions after the adjustment may be insignificant even if the single adjustment factor was applied.
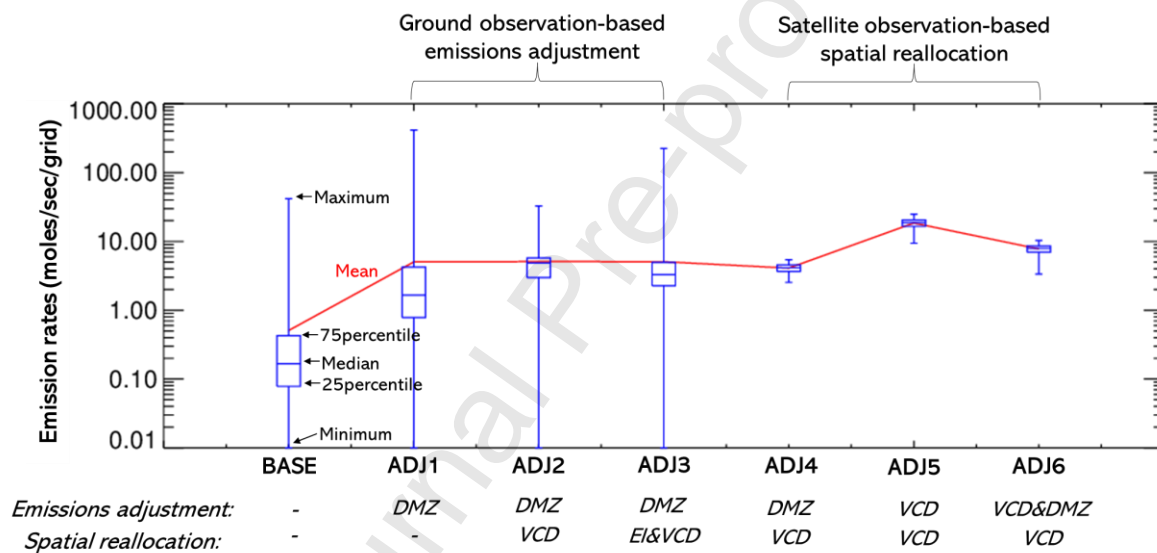
Figure 6. CO emission rates of each grid for the emissions scenario in North Korea. EI, DMZ, and VCD indicate emissions inventory, DMZ observations, and TROPOMI VCD, respectively. DMZ observations were utilized for ADJ1-ADJ4 emissions adjustment, while TROPOMI VCD was for ADJ5. Both DMZ observations and TROPOMI VCD were utilized for ADJ6. TROPOMI VCD was utilized for ADJ2 and ADJ4-ADJ6 for spatial reallocation of emissions, while both emissions inventory and TROPOMI VCD were utilized for ADJ3.

The adjusted CO emissions were spatially reallocated as described in Table 1, except BASE and ADJ1. In ADJ2, the relative ratio of CO emissions between provinces remained the same as in the EI. However, emissions within provinces were reallocated using TROPOMI CO VCD. In Figure 5(c),

21

emissions in Pyongyang were more than five times higher in ADJ2 than in ADJ4, indicating that higher emissions intensity in the bottom-up EI was estimated in the province, probably due to the high population density in the national capital. The ratio of the median to the mean value in ADJ2 emissions was 0.99 (Figure 6), indicating that reallocating emissions make it difficult to distinguish hotspots (i.e., top 10% emission grids) such as power plants and industrial facilities in North Korea, as with ADJ2 emissions. For instance, the ten cities with the highest population in North Korea, according to Kang et al. (2019), are imperceptible in Figure 5(c).

Regarding ADJ3, emissions were reallocated through a hybrid of the spatial distribution of satellite VCD in the North Korean provinces and the information on major emission sources included in the base emissions. Due to the nature of the methodology, the grid locations for the top 10% of emissions in ADJ1 and ADJ3 (Figure 5(b) and 5(d)) were similar. Kang et al. (2019) and Chong et al. (2023) reported that CO emissions are high in Pyongyang and Pukchang, where thermal power plants are located, and in Nampo, where large industrial facilities are located along ports in North Korea. In ADJ1, before the spatial reallocation, two grids around Pyongyang and Sinuiju emitted approximately 10% of the nation's total emissions, equivalent to emissions from 882 grids in rural and mountainous areas that show the lowest emissions. However, the top 8 and the bottom 451 grids accounted for 10% of the nation's total CO emissions after emission reallocation in ADJ3, indicating that unrealistically high emissions from one grid were shared by several grids nearby in the hybrid spatial reallocation (Figure 6). Consequently, the emissions mainly allocated to specific grids before the spatial reallocation decreased. Meanwhile, emissions in suburban and rural areas, where emissions were scarcely allocated due to lack of activity data, increased (Figure 5). Subsequently, the emissions spatially reallocated using various methods were evaluated through air quality simulation as described in the following section.

In ADJ4, the spatial distribution of CO emissions in North Korea was reallocated proportionally to CO VCD in North Korea. The ratio of the mean to the median value in ADJ1 emissions was 3, which implies that a few higher emission grids dominate the national total, as shown in Figure 6. On the

contrary, the mean and median values were similar for ADJ4 emissions (Figure 6). This is because CO emissions from cities such as Pyongyang, Nampo, and Hamheung, characterized by high populations, large power generation, and industrial facilities (Kang et al., 2019), were evenly redistributed nationwide in ADJ4 to obtain monotonous spatial distribution of CO emissions as with that of the satellite VCD. Notably, hotspot emissions in the EI disappeared in ADJ4 (Figure 5(a) and (e)). Because CO has a long residence time in the atmosphere and is affected not only by local emissions but also by emissions in surrounding regions (Kim et al., 2024; Zhou et al., 2021), the horizontal emission gradient allocated with satellite VCD could be weaker than that of the actual emissions. To better spatially allocate emissions in North Korea using satellite VCD, a method that distinguishes the local and transported emission impacts must be considered (Chong et al., 2023).

Similar to ADJ4, CO emissions in ADJ5 and ADJ6 were spatially reallocated using TROPOMI VCD data, as shown in Figure 5(f) and (g). In contrast to CO emissions (i.e., ADJ1) that were distributed based on the pre-gridded EI, the variations in emissions among provinces and hotspots are not noticeable in ADJ5 and ADJ6. Due to the significant difference between the observed and modeled VCDs, the mean value in ADJ5 is the highest among the emission cases in this study. After CO emissions in ADJ5 were refined with DMZ observations, the mean value in ADJ6 decreased but remained higher than those in ADJ3 and ADJ4. As shown in Figure 6, the ranges between minimum and maximum CO emission rates became narrower in the VCD-based emissions adjustments compared to those in the ground observation-based adjustments.

3.4 Comparison to satellite-observed VCD data

The similarity in spatial distribution between the CO VCD of North Korea simulated using the spatially reallocated CO emissions and satellite-observed CO VCD was compared (Figure 7). The CO VCD observed from TROPOMI was higher in the southwest of North Korea, including Pyongyang, than in other parts of the country. As Chong et al. (2023) reported, the satellite VCD in Pyongyang, Pukchang, and Hamheung, where power plants are located, is higher than in nearby areas.

23
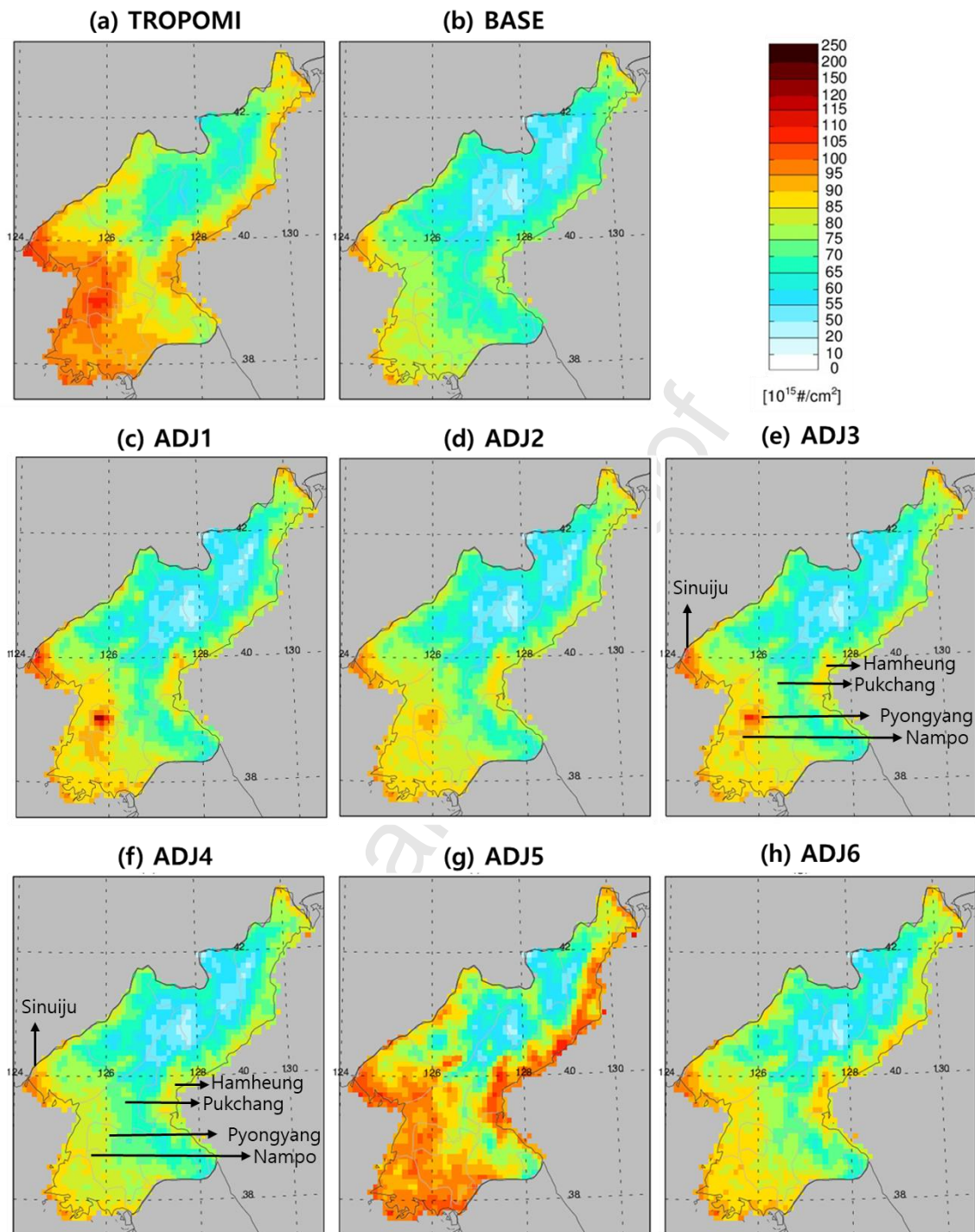
Figure 7. Horizontal spatial distributions of observed and simulated CO VCD during the period of December 2020 to March 2021: (a) TROPOMI, (b) BASE, (c) ADJ1, (d) ADJ2, I ADJ3, (f) ADJ4, (g) ADJ5, and (h) ADJ6.

Since the spatial reallocation of CO emissions was not applied in BASE and ADJ1, the spatial distributions of CO VCD simulated based on the emissions were similar except for the intensity. As

24

can be observed in Figure 7, the simulated VCD is noticeably lower than the observed values. However, after the emissions adjustment as in ADJ1, the simulated VCDs for hotspot areas such as Pyongyang and Sinuiju were higher than those observed. As aforementioned, VCD overprediction, especially in the border area (i.e., Sinuiju), can affect model performance in ground monitoring stations (i.e., Dandong) after the emissions adjustment. Due to this reason, we introduced the spatial reallocation for the adjusted CO emissions in this study. CO emissions in North Korea can increase CO concentrations at Dandong monitoring stations (see Supplementary Data).

After the spatial reallocation, CO VCD hotspots around Pyongyang and Sinuiju decreased (ADJ2–ADJ6 in Figure 7). When TROPOMI CO VCD data were utilized for spatial reallocation, CO emissions became almost flat (Figure 5I-(g)). However, CO VCD simulated with the emissions show spatial variability mainly due to meteorology and terrain influence (Figure 7(f)-(i)). When simulated with the ADJ2 emissions (Figure 5I), CO VCD in Pyongyang and southwestern North Korea increased compared to the CO VCD simulated with ADJ4 emissions because of the high emissions intensity in the provinces in the EI and the provincial level spatial reallocation (Figure 7(d)). CO VCD in Pyongyang simulated with the hybrid spatial reallocation (ADJ3) was as high as that observed. However, the VCD for the other area was lower than that of the satellite observations (Figure 7I). As we utilize the pre-gridded emission data more extensively for reallocation, higher VCD values become more distinct over locally dispersed hotspots (ADJ3 > ADJ2 > ADJ4) when ground observations were utilized for the emissions adjustment.

However, when only the CO VCD was employed for the reallocation, local major emission source locations and intensities remained unclear (i.e., ADJ4). This is because the spatial distribution of CO VCD reflects the combined impacts of local emissions and transboundary transported air pollutants (Chong et al., 2023). Because CO emissions in ADJ5 were reallocated and adjusted using TROPOMI CO VCD, the spatial distribution of the simulated VCD better aligns with the observed data (Figure 7(g)). However, the spatial distribution of VCD apparently decreased when CO emissions in ADJ5 were further adjusted based on DMZ observations (Figure 7(i)).

When the observed VCDs and simulated VCDs by grid were compared in Figure S4, it was found that the relative error decreased by 12% ($= (84.24 - 73.96)/84.24 \times 100\%$) in ADJ1 compared to that of the BASE (17%), and the correlation coefficient (r) improved from 0.94 to 0.97. Regarding ADJ3, the simulation reproducibility was better than those of ADJ2 and ADJ4 as the relative error

25

was 12% and the r value was 0.97 (Figure S4(e)). The mean bias between TROPOMI-observed and modeled VCDs was the lowest in ADJ5, where North Korean CO emissions were adjusted with the satellite-observed VCD (Figure S4(f)). However, when the TROPOMI-derived emissions were further adjusted to better replicate the observed CO concentrations at the DMZ monitoring stations (ADJ6), the mean bias between observed and modeled CO VCDs increased (Figure S4(g)).

3.5 Comparison to ground observations

The emissions adjustment and spatial reallocation method presented in this study were examined by comparing the simulated CO concentrations with those observed from ground monitoring stations adjacent to North Korea, the DMZ in South Korea, and Dandong in China (Figures 8 and S6-7). The mean bias between the simulated and observed concentrations in the DMZ was -68.5 ppb for BASE, with a correlation coefficient of 0.84 for daily mean concentrations (Figure S6(a)). Following the emissions adjustment, the mean biases reduced to -6.7, -11.2, -2.4, -27.3, and 17.5 ppb for ADJ1, ADJ2, ADJ3, ADJ4, and ADJ6, respectively (with corresponding correlation coefficients of 0.89, 0.89, 0.89, 0.87, and 0.89, respectively), indicating improved reproducibility of simulated CO concentrations after the emissions adjustment. Note that the mean bias increased to 145.0 ppb when CO emissions in North Korea were adjusted solely using TROPOMI VCD (ADJ5) due to the larger emission increment in the adjustment compared to other cases. After further adjustment of the emissions utilizing ground observations (ADJ6), the mean bias at the DMZ became similar to other emissions   adjustments.
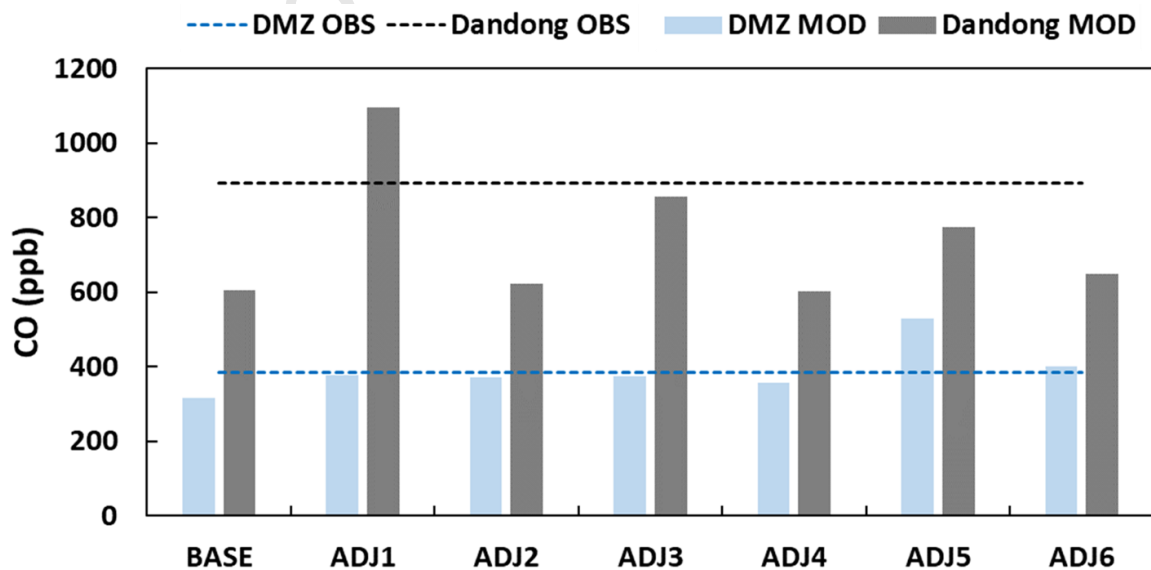
Figure 8. CO concentrations simulated for the demilitarized zone and Dandong monitoring stations before and after emissions adjustment from December 2020 to March 2021.

At the Dandong monitoring stations in China (Figure S7), the BASE simulation underpredicted CO concentrations by -286.2 ppb (with a correlation coefficient of 0.69). After the CO emissions adjustment in North Korea, ADJ1 overpredicted CO concentrations at the stations by 204.3 ppb due to nearby hotspot emissions associated with uncertainty in the spatial distribution of the pre-gridded EI. When spatial reallocation was applied in addition to the emissions adjustment, the mean biases were significantly reduced to -4.9 and -118.2 ppb for ADJ3 and ADJ5, respectively, accompanied by corresponding correlation coefficients of 0.75 and 0.74. This indicates that improving simulation reproducibility is possible through spatial reallocation using observations, such as ground monitors in border areas or satellite VCD, in conjunction with air quality simulation, even when on-site observations are not available. This also suggests that it is important to adjust the total emissions for an area of interest (i.e., North Korea) and to spatially re-distribute the emissions to better reproduce the observed concentration of air pollutants through air quality simulations.

For ADJ2, ADJ4, and ADJ6, their emissions adjustments and reallocations were effective with respect to replicating the observed CO concentrations at DMZ monitoring stations but still resulted in underpredictions of CO concentrations at Dandong stations. However, ADJ3, which utilizes DMZ observations for emissions adjustment and employs a hybrid method for spatial reallocation, effectively replicated the observed CO concentrations at both DMZ and Dandong monitoring stations.

When we altered the sequence of ADJ3 procedures by first applying spatial reallocation of the EI CO emissions using the hybrid method and then adjusting emissions utilizing DMZ observations, we estimated nearly identical changes in emissions (details not provided in the main text). North Korean CO emissions were 11.2 times higher than those in the EI, and the modeled CO biases at DMZ and Dandong monitoring stations were estimated as 0.0 and 14.5 ppb, respectively. The results were also comparable with those obtained using the ADJ3 approach. This suggests that the order of emissions adjustment and spatial reallocation may not always be critical. Instead, the specific data used during each procedure can influence the update of the bottom-up emissions, as demonstrated by the comparison between ADJ2 and ADJ4.

The results in Figures 7 and 8 demonstrate that cross-validation utilizing various data sources, such

as ground and satellite observations, is crucial for updating emissions data and enhancing air quality simulations. This suggests that integrated approaches combining various data sources, including ground and satellite observations, air quality simulations, and emissions inventories, are essential for estimating and cross-validating top-down emissions.

3.6 Discussions on adjusted CO emissions

In this section, we discussed the CO emissions adjustment in ADJ3, which represented observed CO concentrations at both DMZ and Dandong monitoring stations and compared it with findings from previous studies. The adjusted CO emissions in North Korea were 1.5 to 13.3 times higher than those in other bottom-up emissions inventories such as Emissions Database for Global Atmospheric Research (EDGAR) v6.1 (Table S3), indicating that the CO emissions in North Korea, as presented in EIs, are significantly underestimated. Note that the CO emissions in this study were adjusted for winter months only, so different comparisons may arise when estimating emissions for the entire year. One of the advantages of this approach is that CO emissions in North Korea can be re-estimated for different months, seasons, or years to better replicate CO concentrations at the monitoring stations. For instance, the long-term trend of CO emissions in North Korea can be estimated by applying the approach once the observational data become available for a period of interest. However, if observational data is unavailable for a particular month, CO emissions adjusted for that month in different years can be applied without the need for re-estimation, assuming the similarity in monthly and hourly emission patterns. Another example is regarding biomass burning. Irregularly occurring CO emissions from biomass burning within the target area can be estimated when CO concentrations at downwind monitoring stations increase. Evaluation of long-term emission trends can tell how CO emissions from the area of interest have been changing from month to month.

In this study, the ratio of CO emissions in North Korea to those in South Korea increased from 8.5% before the adjustment to 84.8% after the adjustment. The average contributions of North Korean emissions to CO concentrations in South Korea and the DMZ monitoring stations were 2.4 and 6.9 ppb, respectively, before the adjustment. They increased to 23.7 and 73.6 ppb after the adjustment, respectively, corresponding to 4.7 and 19.2% of the average observed CO concentrations in South Korea and the sites during the study period.

Particularly, in the SMA, which has more than half of the South Korean total population and is

close to North Korea, the contribution of North Korean emissions to CO concentrations increased to 44.3 ppb, accounting for 8.0% of the average observed CO concentrations in the area. This implies that if emissions increase in North Korea due to future economic and industrial development, their impact will increase, and the health risk caused by increased exposure to air pollutants will be higher in the densely populated SMA.

In the future, emissions in other areas where ground observations are unavailable can be adjusted by utilizing the concentrations observed in neighboring areas. However, it is important to note that the impact of emission changes significantly diminishes with an increase in distance from the emission source area. Therefore, acquiring observational data near source areas is crucial to effectively apply the emissions adjustment method proposed in this study.

4. Conclusion

In this study, we utilized CO ground observations in border areas, TROPOMI CO VCD data, a pre-gridded bottom-up EI, and air quality simulations to propose a method to adjust and spatially reallocate CO emissions in North Korea, where access to air pollution information, such as ambient measurements and air pollutant emissions, is limited. We began by assessing the uncertainty of CO emissions in North Korea by comparing simulated concentrations with observations at DMZ monitoring stations in the North-South Korean border area. Subsequently, we adjusted and reallocated North Korean CO emissions to minimize the modeled mean biases of CO concentrations at DMZ monitoring stations. We also examined the modeled mean biases at the Dandong monitoring station in the China-North Korea border area in addition to the DMZ monitoring stations to select the optimal method for updating CO emissions in North Korea.

When the VCD alone was used for the emissions adjustment by matching the observed and modeled CO VCD mean values over North Korea, modeled CO concentrations (529 ppb) overpredicted observed ones by 145.0 ppb at DMZ monitoring stations. After refining the adjusted CO emissions utilizing DMZ observations, the mean bias was reduced to 17.5 ppb. As Chong et al. (2023) pointed out, distinguishing between long-range transport impacts and those of local emissions would be necessary to adjust CO emissions solely based on the satellite VCD data.

When North Korean CO emissions were adjusted utilizing DMZ observations, a hybrid method that combines the spatial distributions of pre-gridded bottom-up emissions and satellite VCD data was

applied to reallocate the adjusted CO emissions. Re-simulation with the hybrid method demonstrated the best model performance for CO concentrations at ground monitoring stations near North Korea. The mean biases at the DMZ and Dandong monitoring stations were -2.4 and -4.9 ppb, respectively. Notably, although only DMZ observations were used to adjust emissions in North Korea, simulation reproducibility was also improved at the Dandong monitoring stations. The adjusted CO emissions in North Korea were approximately eleven times higher on average than in the EI chosen during the study period. After emissions adjustment, the North Korean contribution to CO concentrations at the DMZ monitoring stations increased by ten times.

The study findings demonstrate that ground-based and satellite observations, integrated with air quality simulations, can be utilized to improve the bottom-up emissions inventory in areas where air quality data are limited. The emissions adjustment and spatial reallocation method is expected to apply to other areas with high emissions uncertainty. It will also be applicable for estimating other primary air pollutant emissions (i.e., elemental carbon). To this end, it is crucial to secure a monitoring network that can identify the transport of air pollutants between sub-regions, such as the DMZ monitoring stations. Based on this, more accurate emissions can be estimated for areas with high uncertainty, and reliability for neighboring areas' air quality simulation results will be improved. In previous studies, satellite observations were used to remotely estimate emissions. In this study, as an alternative method, we utilized highly resolved ground observations to evaluate and adjust the bottom-up emissions inventory. By accommodating various sources of observations such as satellite, airborne, and ground measurements, it is expected that more accurate emissions can be estimated over more expanded areas. In the future, efforts to harmonize various observations with air quality simulations to better understand and improve emission conditions and air quality in an area of interest will be more diligently demanded.

Declaration of competing interests

The authors declare that they have no known competing financial interests or personal relationships that could have appeared to influence the work reported in this paper.

Declaration of generative AI in scientific writing

During the preparation of this work the author(s) used ChatGPT in order to enhance their English

writing. After using this tool/service, the author(s) reviewed and edited the content as needed and take(s) full responsibility for the content of the publication.

References

Bae, M., Kim, H. C., Kim, B. U., Kim, S., 2018. PM$_{2.5}$ Simulations for the Seoul metropolitan area: (V) Estimation of North Korean emission contribution. J. Kor. Soc. Atmos. Environ. 34(2), 294–305.

Bae, C., Kim, H. C., Kim, B. U., Kim, S., 2020. Surface ozone response to satellite-constrained NOx emission adjustments and its implications. Environ. Pollut. 258, 113469. https://doi.org/10.1016/j.envpol.2019.113469

Cho, J. H., Kim, H. S., Yoon, M. B., 2022. The influence of atmospheric blocking on regional PM10 aerosol transport to South Korea during February–March of 2019. Atmos. Environ. 277, 119056. https://doi.org/10.1016/j.atmosenv.2022.119056

Choi, Y., Kanaya, Y., Park, S. M., Matsuki, A., Sadanaga, Y., Kim, S. W., Uno, I., Pan, X., Lee, M., Kim, H., Jung, D. H., 2020. Regional variability in black carbon and carbon monoxide ratio from long-term observations over East Asia: assessment of representativeness for black carbon (BC) and carbon monoxide (CO) emission inventories. Atmos. Chem. Phys. 20(1),83–98. https://doi.org/10.5194/acp-20-83-2020

Chong, H., Lee, S., Cho, Y., Kim, J., Koo, J.-H., Pyo Kim, Y., Kim, Y., Woo, J.-H., Hyun Ahn, D., 2023. Assessment of air quality in North Korea from satellite observations. Environ. Intl. 171, 107708. https://doi.org/10.1016/j.envint.2022.107708

Cooper, M., Martin, R. V., Padmanabhan, A., Henze, D. K., 2017. Comparing mass balance and adjoint methods for inverse modeling of nitrogen dioxide columns for global nitrogen oxide emissions. J. Geophys. Res. Atmos. 122(8), 4718–4734. https://doi.org/10.1002/2016JD025985

Crippa, M., Janssens-Maenhout, G., Guizzardi, D., Van Dingenen, R., Dentener, F., 2019. Contribution and uncertainty of sectorial and regional emissions to regional and global $PM_{2.5}$ health impacts. Atmos. Chem. Phys. 19(7), 5165–5186. https://doi.org/10.5194/acp-19-5165-2019

Egerstrom, N., Rojas-Rueda, D., Martuzzi, M., Jalaludin, B., Nieuwenhuijsen, M., So, R., Lim, Y. H., Loft, S., Andersen, Z. J., Cole-Hunter, T., 2023. Health and economic benefits of meeting WHO air quality guidelines, Western Pacific Region. Bull World Health Organ, 101(2), 130–139. https://doi:10.2471/BLT.22.288938

Emery, C., Tai, E., Yarwood, G., 2001. Enhanced meteorological modeling and performance evaluation for two Texas ozone episodes. Prepared for the Texas Natural Resource Conservation Commission by ENVIRON International Corporation.

Feng, S., Jiang, F., Wu, Z., Wang, H., Ju, W., Wang, H., 2020. CO emissions inferred from surface CO observations over China in December 2013 and 2017. J. Geophys. Res. Atmos. 125(7), e2019JD031808. https://doi.org/10.1029/2019JD031808

Itahashi, S., Yamamura, Y., Wang, Z., Uno, I., 2022. Returning long-range $PM_{2.5}$ transport into the leeward of East Asia in 2021 after Chinese economic recovery from the COVID-19 pandemic. Sci. Rep. 12(1), 5539. https://doi.org/10.1038/s41598-022-

09388-2

Jo, Y. J., Lee, H. J., Jo, H. Y., Woo, J. H., Kim, Y., Lee, T., Heo, G., Park, S. M., Jung, D., Park J, Kim, C. H., 2020. Changes in inorganic aerosol compositions over the Yellow Sea area from the impact of Chinese emissions mitigation. Atmos. Res. 240, 104948. https://doi.org/10.1016/j.atmosres.2020.104948

Kang, S., Choi, J., Yoon, H., Choi, W., 2019. Changes in the extent and distribution of urban land cover in the Democratic People's Republic of Korea (North Korea) between 1987 and 2010. Land Degrad. Develop. 30(16), 2009–2017.

Kang, Y. H., Son, K., Kim, B. U., Chang, Y., Kim, H. C., Schwarz, J. P., Kim, S., 2023. Adjusting elemental carbon emissions in Northeast Asia using observed surface concentrations of downwind area and simulated contributions. Environ. Intl. 178, 108069. https://doi.org/10.1016/j.envint.2023.108069

Kim, N. K., Kim, Y. P., Morino, Y., Kurokawa, J. I., Ohara, T., 2014. Verification of NOx emission inventories over North Korea. Environ. Pollut. 195, 236–244. https://doi.org/10.1016/j.envpol.2014.06.034

Kim, I. S., Lee, J. Y., Wee, D., Kim, Y. P., 2019a. Estimation of the contribution of biomass fuel burning activities in North Korea to the air quality in Seoul, South Korea: Application of the 3D-PSCF method. Atmos. Res. 230, 104628. https://doi.org/10.1016/j.atmosres.2019.104628

Kim, I. S., Kim, Y. P., 2019b. Characteristics of energy usage and emissions of air pollutants in North Korea. J. Kor. Soc. Atmos. Environ. (Korean) 35(1), 125–137.

Kim, H. C., Kim, S., Cohen, M., Bae, C., Lee, D., Saylor, R., Bae, M., Kim, E., Kim, B.U., Yoon, J.H., Stein, A., 2021. Quantitative assessment of changes in surface particulate matter concentrations and precursor emissions over China during the

COVID-19 pandemic and their implications for Chinese economic activity. Atmos. Chem. Phys. 21(13), 10065–10080. https://doi.org/10.5194/acp-21-10065-2021

Kim, D. Y., de Foy, B., Kim, H., 2022. The investigations on organic sources and inorganic formation processes and their implications on haze during late winter in Seoul, Korea. Environ. Res. 212, 113174. https://doi.org/10.1016/j.envres.2022.113174

Kim, E., Kim, H. C., Kim, B. U., Woo, J., Liu, Y., Kim, S., 2024. Development of Surface Observation-Based Two-Step Emissions Adjustment and its Application on Co, NOx, and SO_2 Emissions in China and South Korea. NOx, and SO_2 Emissions in China and South Korea.

Kim, E., Kim, B. U., Kang, Y. H., Kim, H. C., Kim, S., 2023. Role of vertical advection and diffusion in long-range $PM_{2.5}$ transport in Northeast Asia. Environ. Pollut. 320, 120997. https://doi.org/10.1016/j.envpol.2022.120997

Kong, H., Lin, J., Chen, L., Zhang, Y., Yan, Y., Liu, M., Ni, R., Liu, Z., Weng, H., 2022. Considerable Unaccounted Local Sources of NOx Emissions in China revealed from satellite. Environ. Sci. Technol. 56(11), 7131-7142. https://doi.org/10.1021/acs.est.1c07723

Kurokawa, J., Ohara, T., 2020. Long-term historical trends in air pollutant emissions in Asia: Regional emission inventory in ASia (REAS) version 3. Atmos. Chem. Phys. 20(21), 12761–12793. https://doi.org/10.5194/acp-20-12761-2020

Lamsal, L. N., Martin, R. V., Padmanabhan, A., Van Donkelaar, A., Zhang, Q., Sioris, C. E., Chance, K., Kurosu, T.P., Newchurch, M. J., 2011. Application of satellite observations for timely updates to global anthropogenic NOx emission inventories. Geophys. Res. Lett. 38(5). https://doi.org/10.1029/2010GL046476

Lee, H. J., Jo, H. Y., Kim, S. W., Park, M. S., Kim, C. H., 2019. Impacts of atmospheric

vertical structures on transboundary aerosol transport from China to South Korea. Sci. Rep. 9(1), 13040. https://doi.org/10.1038/s41598-019-49691-z

Lee, K., Lim, Y.H., Choi, Y.J., Kim, S., Bae, H.J., Han, C., Lee, Y.A., Hong, Y. C. (2020). Prenatal exposure to traffic-related air pollution and risk of congenital diseases in South Korea. Environ. Res. 191, 110060. https://doi.org/10.1016/j.envres.2020.110060

Li, M., Zhang, Q., Kurokawa, J. I., Woo, J. H., He, K., Lu, Z., Ohara, T., Song, Y., Streets, D.G., Carmichael, G.R., Zheng, B., 2017. MIX: a mosaic Asian anthropogenic emission inventory under the international collaboration framework of the MICS-Asia and HTAP. Atmos. Chem. Phys. 17(2), 935–963. https://doi.org/10.5194/acp-17-935-2017

Li, B., Shi, X., Jiang, J., Lu, L., Ma, L. X., Zhang, W., Wang, K., Qi, H., 2023. Understanding the inter-city causality and regional transport of atmospheric $PM_{2.5}$ pollution in winter in the Harbin-Changchun megalopolis in China: A perspective from local and regional. Environ. Res. 222, 115360. https://doi.org/10.1016/j.envres.2023.115360

Li, H., Zheng, B., Ciais, P., Boersma, K. F., Riess, T., Martin, R. V., Broquet, G., van der A, R., Li, H., Hong, C., He, K., 2023. Satellite reveals a steep decline in China's CO_2 emissions in early 2022. Sci. Adv. 9(29), eadg7429. https://doi:10.1126/sciadv.adg7429

Byun, D., Schere, K.l., 2006. Review of the governing equations, computational algorithms, and other components of the Models-3 Community Multi-scale Air Quality (CMAQ) Modeling System. Appl. Mechan. Rev. 59(2), 51–77.

Byun, D.W., Kim, S.T., Kim, S.B., 2007. Evaluation of air quality models for the simulation of a high ozone episode in the Houston metropolitan area. Atmos. Environ. 41(4),

837–853.

Jiang, Z., Worden, J.R., Worden, H., Deeter, M., Jones, D., Arellano, A.F., Henze, D.K., 2017. A 15-year record of CO emissions constrained by MOPITT CO observations. Atmos. Chem. Phys. 17(7), 4565–4583.

Li, H., Zheng, B., Ciais, P., Boersma, K.F., Riess, T.C.V., Martin, R.V., Broquet, G., van der A, R., Li, H., Hong, C. and Lei, Y., 2023. Satellite reveals a steep decline in China's CO(2) emissions in early 2022. Sci. Adv, 9(29), eadg7429.

Petetin, H., Sauvage, B., Parrington, M., Clark, H., Fontaine, A., Athier, G., Blot, R., Boulanger, D., Cousin, J.M., Nédélec, P., Thouret, V., 2018. The role of biomass burning as derived from the tropospheric CO vertical profiles measured by IAGOS aircraft in 2002–2017. Atmos. Chem. Phys. 18(23), 17277–17306.

Oh, J., Choi, S., Han, C., Lee, D.W., Ha, E., Kim, S., Bae, H.J., Pyun, W.B., Hong, Y.C., Lim, Y. H., 2023. Association of long-term exposure to $PM_{2.5}$ and survival following ischemic heart disease. Environ. Res. 216, 114440. https://doi.org/10.1016/j.envres.2022.114440

Park, J., Jung, J., Choi, Y., Lim, H., Kim, M., Lee, K., Lee Y.G., Kim, J., 2023. Satellite-based, top-down approach for the adjustment of aerosol precursor emissions over East Asia: the TROPOspheric Monitoring Instrument (TROPOMI) NO 2 product and the Geostationary Environment Monitoring Spectrometer (GEMS) aerosol optical depth (AOD) data fusion product and its proxy. Atmos. Meas. Tech. 16(12), 3039–3057. https://doi.org/10.5194/amt-16-3039-2023

Pendergrass, D. C., Zhai, S., Kim, J., Koo, J. H., Lee, S., Bae, M., Kim, S., Liao, H., Jacob, D. J., 2022. Continuous mapping of fine particulate matter ($PM_{2.5}$) air quality in East Asia at daily 6×6 km^2 resolution by application of a random forest algorithm to

2011–2019 GOCI geostationary satellite data. Atmos. Meas. Tech. 15(4), 1075–1091. https://doi.org/10.5194/amt-15-1075-2022

WHO, 2022. World Health Statistics 2020: Monitoring health for SDGs. https://apps.who.int/iris/bitstream/handle/10665/332070/9789240005105-eng.pdf?sequence=1&isAllowed=y

Woo, J. H., Baek, J. M., Kim, J. W., Carmichael, G. R., Thongboonchoo, N., Kim, S. T., An, J. H. (2003). Development of a multi-resolution emission inventory and its impact on sulfur distribution for Northeast Asia. Water Air Soil Pollut. 148, 259–278.

Woo, J. H., Kim, Y., Kim, H. K., Choi, K. C., Eum, J. H., Lee, J. B., Lim J.H., Kim, J., Seong, M., 2020. Development of the CREATE inventory in support of integrated climate and air quality modeling for Asia. Sustainability 12(19), 7930. https://doi.org/10.3390/su12197930

Xia, Y., Zhao, Y., Nielsen, C. P., 2016. Benefits of China's efforts in gaseous pollutant control indicated by the bottom-up emissions and satellite observations 2000–2014. Atmos. Environ. 136, 43–53. https://doi.org/10.1016/j.atmosenv.2016.04.013

Yeo, M. J., Kim, Y. P., 2018. Electricity supply trend and operating statuses of coal-fired power plants in North Korea using the facility-specific data produced by North Korea: characterization and recommendations. Air Quality, Atmos. Health 11, 979–992. https://doi.org/10.1007/s11869-018-0601-5

Yeo, M. J., Kim, Y. P., 2019. The state of the air quality and measures for improving it in North Korea. J. Korean Soc. Atmos. Environ. (Korean) 35(3), 318–335. https://doi.org/10.5572/KOSAE.2019.35.3.318

Zhou, M., Jiang, J., Langerock, B., Dils, B., Sha, M. K., Mazière, M. D., 2021. Change of CO concentration due to the COVID-19 lockdown in China observed by surface and

satellite observations. Remote Sens. 13(6), 1129.

https://doi.org/10.3390/rs13061129

Graphical Abstract
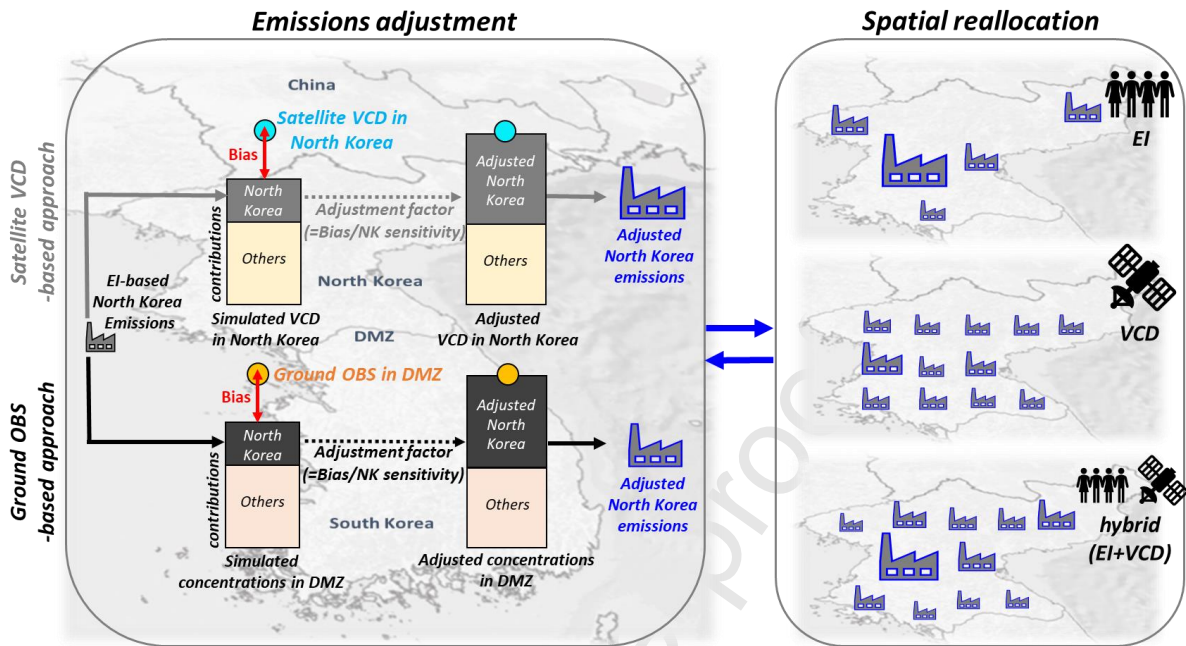
Fig. Conceptual diagram for adjusting and reallocating emissions in North Korea.

40

Highlights

- A new method was proposed to optimally adjust CO emissions in North Korea

- CO emissions were adjusted using ground observations from demilitarized zone (DMZ)

- Adjusted CO emissions were 10.9 times higher than those in the bottom-up EIs

- Harmonizing both ground and satellite observations enhanced emission reconstruction

- The model performances of CO concentrations were improved in both DMZ and China